



Study for the types of functional molecules to the effect of surface properties of ZnO nanorods

Journal:	<i>RSC Advances</i>
Manuscript ID:	RA-ART-10-2014-012889
Article Type:	Paper
Date Submitted by the Author:	22-Oct-2014
Complete List of Authors:	Wang, Lei; Liaocheng University, Feng, Lu; Liaocheng University, Liu, Jifeng; Liaocheng University,

Cite this: DOI: 10.1039/c0xx00000x

www.rsc.org/xxxxxx

ARTICLE TYPE

Study for the types of functional molecules to the effect of surface properties of ZnO nanorods

Lei Wang,* Lu Feng and Jifeng Liu

Received (in XXX, XXX) Xth XXXXXXXXX 20XX, Accepted Xth XXXXXXXXX 20XX

DOI: 10.1039/b000000x

In this work, surface modification of ZnO nanorods were carried out with three types of organic molecules that concluded ethylenediamine, sodium citrate and butanethiol to better understand the surface properties of ZnO nanorods. FT-IR spectra were used to characterize the surface modification of ZnO nanorods. Photoluminescence spectra and electrochemiluminescence spectra were applied to study the influence of the functional molecule structure to the surface electron structures and the surface band gap of ZnO nanorods. The result indicated that the surface state of ZnO nanorods may be regulated by the selection of functional organic molecules. It contributes to an understanding of organic - inorganic interfaces and surface properties and may be useful for the design of novel multiplexing sensors or photovoltaic-hybrid materials and the corrosion prevention of ZnO nanostructures.

1. Introduction

ZnO is an important wide-bandgap semiconductor that possesses a rich family of nanostructures. Extensive researches on synthesis, characterization, and applications of ZnO have been carried out due to their useful properties such as piezoelectricity, conductivity, optical absorption and emission, high voltage-current nonlinearity, sensitivity to gases and chemical agents, and catalytic activity.¹ It has been reported that the morphology features have a crucial role to the properties of the prepared ZnO and influence their applications.²⁻⁴ Surface modification that based on self-assembled and covalently bonded organic monolayers can be used to manipulate surface properties. Functionalizations of metal oxides may be beneficial due to their applications in manipulating surface properties and have been widely investigated due to the importance of these materials in several hybrid inorganic-organic electronic applications.^{5, 6} These hybrid materials have taken the form of bulk, film, nanoparticles, and molecularly thin self-assembled monolayers that have proven to be versatile in terms of the new properties that can bring to surfaces and interfaces.^{7, 8} Because organic molecules are known to either promote or inhibit the crystal growth of ZnO, the attachment of organic molecules to ZnO also can be used to modify the surface properties of ZnO nanostructures.^{9, 10} Photoluminescence (PL) and X-ray absorption spectroscopies evidenced that the electronic configuration of ZnO nanoparticles were altered by surface modification, which depended on the particular molecule.^{10, 11} Surface modification and efficacy of ZnO nanoparticles may be influenced by the chemical and physical properties of molecular anchors.^{7, 9, 12}

Department of Chemistry, Liaocheng University, Liaocheng, 252059, Shandong, China. Tel & Fax: +86-635-8239001
Email: wangl@ustc.edu

Surface passivation has been achieved using organic capping agents,^{13, 14} such surface states can act as quenchers of the luminescence, and the passivation of the surface is the key to the preparation of highly luminescent semiconductor nanocrystals.^{15, 16} The bandgap of ZnO nanocrystals can be controlled by the surface functional molecule and then contribute to the the fabrication of conventional organic photovoltaic devices.¹⁷

In this work, ZnO nanorods were prepared with hydrothermal synthesis. Ethylenediamine, sodium citrate and butanethiol were used as molecular anchors to modify the surface properties of ZnO nanorods. Fourier transform infrared (FT-IR) spectra were used to investigate the surface composition as the functional molecule reacted with surface Zn atom. PL spectra and electrochemiluminescence (ECL) spectra were applied to study the effect of surface functionalization on the surface band gaps of ZnO nanorods. It was shown that the surface state of ZnO nanostructures can be regulated by enabling selective functional molecule. This work may be helpful in understanding the organic-inorganic interfaces and surface properties and may be useful for the design of novel multiplexing sensors and the corrosion prevention of ZnO nanostructures.

2. Experimental Section

2.1 Chemicals

Zinc acetate ($\text{Zn}(\text{Ac})_2 \cdot 2\text{H}_2\text{O}$), potassium chloride (KCl), potassium hydroxide (KOH), potassium peroxydisulfate ($\text{K}_2\text{S}_2\text{O}_8$), sodium hydroxide (NaOH), glycol, butanethiol, sodium citrate, ethylenediamine and ethanol were purchased from Sinopharm Chemical Regent Co., Ltd. (Shanghai, China). All chemical reagents were of analytical grade and used without further purification. Water used in this work was prepared from Milli-Q water purification system ($\geq 18 \text{ M}\Omega$).

2.2 Apparatus

The morphology and crystal structure of as-prepared products were characterized with Sirion 200 Field Emission Scanning Electron Microscope (FE-SEM, FEI, Netherlands) equipped with an INCA Energy Dispersive Spectrometer (EDS, Oxford Instruments, the United Kingdom).

The composition and phase of ZnO nanostructures were acquired by X-Ray Diffraction (XRD) with a D8 Advance powder X-ray diffractometer (XRD, Bruker, German) using Cu K α radiation ($\lambda = 0.15406$ nm). The surface functionalizations of ZnO nanorods with organic molecules were characterized by FT-IR (Thermo Electron Corporation, the United States).

The PL spectra of the as-prepared products were measured with a FLS 920 fluorescence spectrometer (Edinburgh Instruments Ltd., the United Kingdom) equipped with a red sensitive PMT (R928-P) at room temperature. All PL spectra were acquired using a Xe 900 lamp with an excitation wavelength of 325 nm at room temperature, excitation slit and emission slit were 1.0 nm. For ECL spectra measurement, emission scan mode was performed to record the signals of ECL signal.

2.3 Preparation of ZnO nanorods

ZnO nanorods were prepared by hydrothermal method. 0.33g of Zn(Ac)₂·2H₂O was dissolved in 5.0 mL of 6 mol L⁻¹ NaOH solution, and then 10 mL of glycol was successively dropped into the mixture. After stirring for 15 min, the mixture was transferred into a Teflon-lined stainless-steel autoclave kept at 150 °C for 8 h. The products were collected by centrifugation, washed with water and then dried.

2.4 Surface modification of ZnO nanorods

2.4.1 Surface modification of ZnO nanorods with sodium citrate

It was well known that ZnO crystals synthesized by hydrothermal method in the presence of citrate present large areas of (0001) faces. In this work, the citrate adsorption on the surface of ZnO nanorods was carried out as following: the prepared ZnO nanorods were immersed into 100 mmol L⁻¹ sodium citrate solution, dispersed by stirring and then kept for 1 day. The obtained sample was then washed to remove excess reactants and dried. Due to the strong chelating bonds between carboxylates and Zn atoms on the surface,^{18, 19} citrate molecules were chemisorbed onto the surface of ZnO nanorods and formed a dense self-assembled monolayer on the surface of ZnO nanorods.

2.4.2 Surface modification of ZnO nanorods with ethylenediamine

As reported earlier, ZnO nanocrystals with large areas of (100) plane have been grown in the presence of ethylenediamine. ethylenediamine adsorbs much more strongly to the (100) surface than the (001) surface of ZnO.²⁰ In this study, ZnO nanorods were added into 100 mmol L⁻¹ ethylenediamine solution and uniformly dispersed by stirring. And then the mixture was kept in room temperature for 1 day. The obtained sample was then washed to remove excess reactants and dried for measurement.

2.4.3 Surface modification of ZnO nanorods with butanethiol

The process to encapsulate ZnO nanorods with butanethiol was carried out as reported.²¹ Before use, the prepared ZnO nanorods were dried at 200 °C for about 24h, and then 0.60g of the dried ZnO nanorods were added into 200 mL of 95% ethanol solution.

After ultrasonic dispersing, the suspended solution was stirred at 65 °C for 1 h. 300 mg (about 0.33 mM) of butanethiol was added into the solution, sonicated for 5 min, and then stirred for another 1 h at 65 °C. The product was centrifuged, washed extensively with 100% ethanol, and dried in a vacuum oven.

2.5 Electrochemiluminescence Measurement

For ZnO samples modified with different organic molecules, 2.0 μ L of 1 mg mL⁻¹ well-dispersed sample suspension was dropped onto the surface of ITO, dried in air and then used as the working electrode (WE).

All electrochemical measurements were conducted on a CHI 760B electrochemical workstation (Shanghai Chenhua Co., China) and performed in a quartz cell. Ag/AgCl electrode and platinum wire (0.5 mm in diameter) were employed as the reference (RE) and the counter electrodes (CE) respectively. All potentials in this work were given versus the Ag/AgCl electrode. Cyclic voltammetry (CV) and ECL studies were performed with a RFL-1 ultraweak chemiluminescence/bioluminescence analyzer system (Xian Remax Analysis Instrument Co. Ltd., Xi'an, China) and the PMT was biased at 800V.

3. Results and Discussion

3.1 Morphology and Structure Characterization

FE-SEM image of prepared ZnO nanorods was shown in Fig 1a. It was shown that the prepared ZnO nanorods were about 1.35 μ m in length and 0.28 μ m in diameter, the surface of ZnO nanorods were smooth. However, the surface of ZnO nanorods roughened as ZnO nanorods were modified with ethylenediamine and sodium citrate (Fig 1b,c) and certain level agglomeration appeared for ZnO nanorods functionalized with butanethiol (Fig 1d).

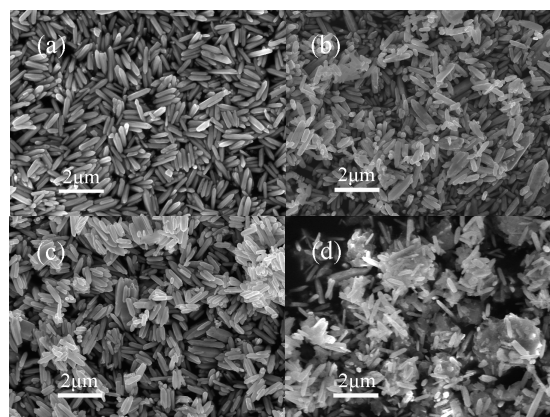


Fig 1 FE-SEM of (a) ZnO nanorods, (b) ethylenediamine-ZnO nanorods, (c) citrate-ZnO nanorods, (d) butanethiol-ZnO nanorods

The chemical composition of obtained products was characterized by EDS (Fig 2). Fig 2a confirms the existence of ZnO. For ZnO nanorods modified with ethylenediamine, the N element in ethylenediamine molecules was not found in EDS image (Fig 2b) because N element is one of light elements that can't be detected by common EDS instrument. For ZnO nanorods modified with citrate, the elements that can be detected only contained O and Zn (Fig 2c). For ZnO nanorods functionalized with butanethiol, the emergence of S element in EDS image (Fig

2d) indicated that butanethiol molecules were chemically bonded onto the surface of ZnO nanorods.

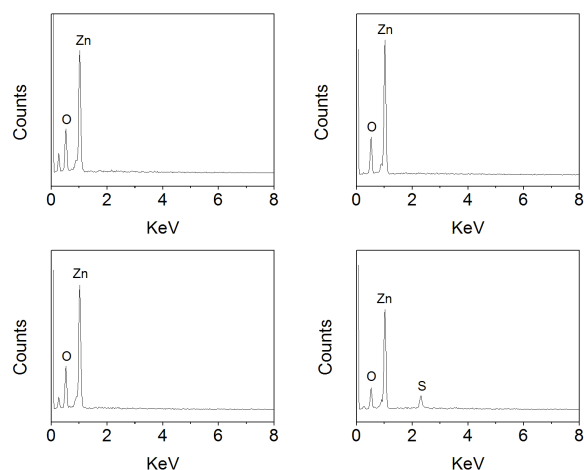


Fig 2 EDS of (a) ZnO nanorods, (b) ethylenediamine-ZnO nanorods, (c) citrate-ZnO nanorods, (d) butanethiol-ZnO nanorods

The XRD patterns of as-prepared ZnO samples were shown in Fig 3. It demonstrated that the prepared sample is crystalline, and all the diffraction peaks in the pattern can be indexed as hexagonal wurtzite-structure ZnO (JCPDS NO. 36-1451).²²

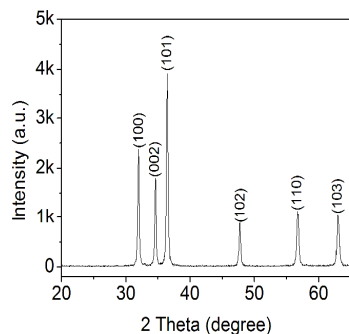


Fig 3 XRD patterns of ZnO nanorods

3.2 FT-IR Measurement of Functionalized ZnO nanorods

FTIR has previously been used to probe the interactions between small molecules and mineral surfaces.²⁰ The adsorption of various carboxylic acids on slurries of different alumina-silicates has been studied, and the observed IR spectra were correlated with theoretically calculated spectra for different bonding arrangements of the functional groups.²³ For this work, the nature of the surface functionalization of ZnO nanorods were investigated by FT-IR spectroscopy and interpreted on the basis of previously reported studies on the anchoring of organic ligands onto the surface of oxides.²⁴⁻²⁸

The typical IR spectrum of ZnO nanorods is shown in the 2000-400 cm^{-1} region (Fig 4a). The observed peaks at 564 and 406 cm^{-1} were the characteristic stretching of Zn-O bonds in zinc oxide.¹⁶

The IR spectrum of ethylenediamine and ethylenediamine adsorption on ZnO nanorods was shown in Fig 4b. The peak at 1595 cm^{-1} originated from the scissoring of NH_2 group, while the peaks present at 1524, 1476 and 1378 cm^{-1} can be attributed to the scissoring vibration, out-of-plane deformation vibration, and

wagging vibration of the methylene groups, respectively. The dramatic change in the IR spectra of ethylenediamine adsorbed on ZnO nanorods compared to pure ethylenediamine may be resulted from the lone pair of electrons on both amine groups of ethylenediamine complex with the (100) plane of ZnO.

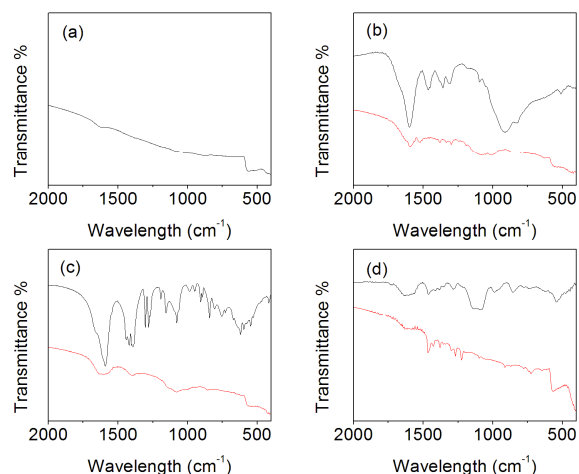


Fig 4 FT-IR spectra of (a) ZnO nanorods, (b) ethylenediamine (up) and ethylenediamine-ZnO nanorods (down), (c) sodium citrate (up) and citrate-ZnO nanorods (down), (d) butanethiol (up) and butanethiol-ZnO nanorods (down)

The spectrum of sodium citrate and citrate adsorbed on ZnO nanorods was shown in Fig. 4c. Two characteristic bands centered at 1585 cm^{-1} and 1393 cm^{-1} can be attributed to the antisymmetric and symmetric stretching vibrations of carboxylate groups complexed with surface Zn centers dominated in the spectra of the nanocrystals^{24, 25}, respectively. The wavenumber value of COO^- antisymmetric stretch of citrate adsorbed on ZnO nanorods is considerably higher than that in the corresponding pure citrate salt, the variation may result from the formation of complex between carboxylic acid and zinc atoms. The mode of binding of carboxylate adsorbates onto the ZnO surface might be interpreted as being unidentate. The peak at 1250 cm^{-1} is attributed to a combination of methylene (CH_2) wagging and twisting vibrations. The large shift in wavenumber (ca. 20 cm^{-1}) may also result from the surface bind interaction between citrate and ZnO and the formation of carboxylate complexed structures.

The IR spectrum of butanethiol and butanethiol adsorption on ZnO nanorods was shown in Fig. 4d. The medium strong peak at 1464 cm^{-1} corresponded to the scissoring vibration of methylene groups in the butanethiol. The weak peaks appeared at 788 cm^{-1} and 744 cm^{-1} came from the C-S scissoring vibration. The surface functionalization of ZnO nanorods may result from the formation of zinc-thiol complexes during the thiol grafting reaction as butanethiol molecules reacted at the hydroxylated sites of zinc oxide lattice (ZnO-OH).^{21, 29} The IR spectra variation of ZnO nanorods modified with butanethiol compared to pure butanethiol may be resulted from the formation of zinc-thiol complexes on the (100) plane of ZnO nanorods.

3.3 PL spectra of functionalized ZnO nanorods

It has been reported that PL spectra of ZnO nanostructures originated from the defect emissions that exhibited a strong

dependence on the fabrication conditions, annealing atmosphere and temperature, and excitation wavelength.³⁰⁻³² In this work, the optical properties of excitonic recombinations in ZnO nanorods functionalized with organic molecules were investigated by PL measurements at room temperature, the maximum PL wavelength of ZnO nanorods, ethylenediamine-ZnO nanorods, citrate-ZnO nanorods, and butanethiol-ZnO nanorods were 505, 493, 491 and 487nm, respectively.

In order to obtain useful information, the PL spectra of ZnO nanorods functionalized with organic molecules were analyzed, as shown in Fig. 4. For ZnO nanorods, the PL emission spectrum can be decomposed into three Gaussian components centred in 395nm, 503nm, and 592 nm by fitting with the Gaussian function (Fig.5a). However, the PL emission spectrum of ZnO nanorods modified with ethylenediamine can be decomposed into three Gaussian components centred in 395nm, 492nm, and 592 nm by fitting with the Gaussian function (Fig.5b). The PL emission spectrum of ZnO nanowires modified with citrate can be decomposed into three Gaussian components centred in 395nm, 493nm, and 570 nm by fitting with the Gaussian function (Fig.5c). The PL emission spectrum of ZnO nanowires modified with 1-butanethiol also can be decomposed into three Gaussian components centred in 395nm, 493nm and 600 nm (Fig.5d). Three emitting bands, which include a weak ultraviolet emission, a strong green light emission and a broad yellow-orange light emission, can be observed. The UV emission corresponds to the near band edge (NBE) emission of the wide band-gap of ZnO originated from the direct recombination of free excitons in the nanostructures. The green emissions are likely due to donor acceptor transitions involving defect complexes,³¹ the blue shift of green light emission from ZnO nanorods modified with organic molecules may contribute to the formation of complexes between the Zn atoms on the surface of ZnO nanorods and the $-NH_2$ in ethylenediamine, the $-COO^-$ in citrate and $-SH$ in butanethiol. The broad yellow-orange emission band in the visible region is commonly referred to deep-level or trap-state emission resulted from the recombination of a photogenerated hole with a charge state of the specific defect, such as oxygen vacancies, or resulted from the surface deep traps. The decomposed maximum emission wavelength of ZnO nanorods modified with ethylenediamine is roughly the same as that from ZnO nanorods, while the decomposed maximum emission wavelength of ZnO nanorods modified with citrate is blue-shifted and the maximum emission band of ZnO nanorods modified with butanethiol is red-shifted compared to that from ZnO nanorods. The result indicated that the type of functional molecules may influence the position of maximum emission peaks of yellow-orange emission bands, which means that the deep-level or trap-state of ZnO surface will be influenced by the types of bonded organic molecules. Because PL mainly occurs through excitation and emission within the nanocrystal core³³ and PL peaks can be assigned to surface state and phonon-assisted recombination,³⁴ surface modification of ZnO nanorods with organic molecules reduced the density of oxygen vacancies near the surfaces, while the low concentration of defects will suppress the deep-level emission.³⁵ Because the electron and hole wave functions can interact strongly with the nanocrystal surface, surface modification may be able to change the surface state of ZnO

nanorods and then influence the radiative recombination between deep levels formed by oxygen vacancies and free holes.³⁵

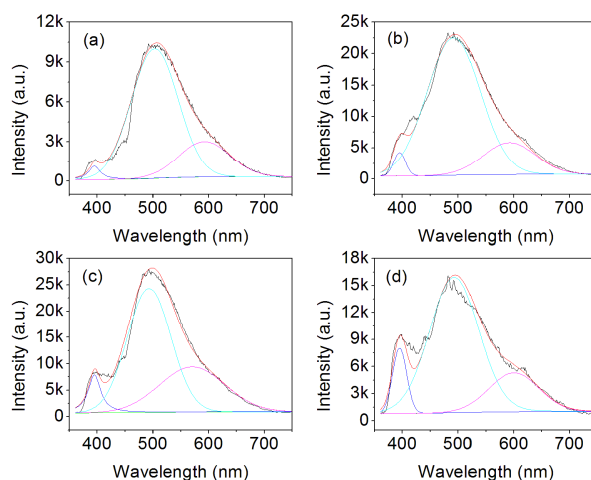


Fig 5 PL spectra of (a) ZnO nanorods, (b) ethylenediamine-ZnO nanorods, (c) citrate-ZnO nanorods, (d) butanethiol-ZnO nanorods

3.4 ECL emission of functionalized ZnO nanorods

ECL emission measurements of ZnO modified with different organic molecules were carried out with CV in the solution containing 0.1M KOH, 0.1M $K_2S_2O_8$ and 0.1M KCl as reported. In ECL measurement, ZnO nanostructures were the only electroactive and luminescence species present on the surface of WE. Therefore, the ECL emission was generated from the reaction of ZnO with the co-reactant of $S_2O_8^{2-}$ in the solution. Functional ZnO nanorods coated ITO was used as WE directly. The potential scan region of 0 to -2.0 V was selected to display the ECL characteristics of as-prepared samples. It was shown that when consecutive scans from 0 to -2.0 V at a scan rate of 100 $mV s^{-1}$ were performed in 1600s, ZnO nanorods coated ITO and functional ZnO nanorods coated ITO present stable ECL signals (Fig 6).

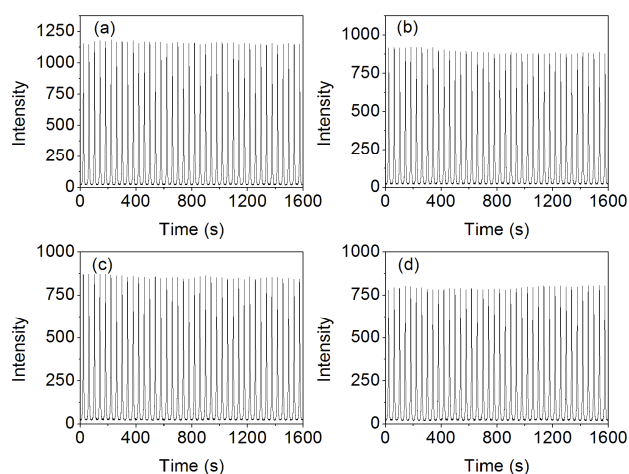


Fig 6 ECL emission of (a) ZnO nanorods, (b) ethylenediamine-ZnO nanorods, (c) citrate-ZnO nanorods, (d) butanethiol-ZnO nanorods

The results indicated that the ECL intensity decreased gradually from ZnO nanorods to ethylenediamine-ZnO nanorods, citrate-ZnO nanorods and butanethiol-ZnO nanorods, which means that

surface modification by organic molecules changed the surface state of ZnO nanorods and then influence the recombination efficiency of conduction band electron and valence band hole. The difference of ECL intensity generated from ethylenediamine-

3.5 ECL spectra of functionalized ZnO nanorods

For ECL spectra measurement, pulsed potential was continuously applied to the working electrodes from 0 to -2.0 V within 1s pulse width. The real-time ECL spectra were shown in Fig 7. The results indicated that the maximum ECL emission wavelengths were 634 nm for ZnO nanorods, 617 nm for ethylenediamine-

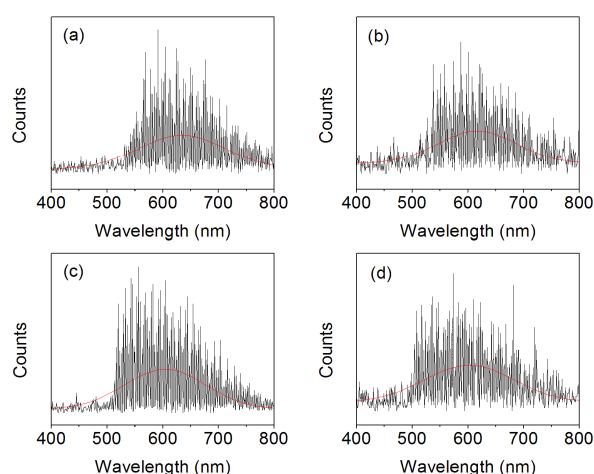


Fig 7 ECL spectra of (a) ZnO nanorods, (b) ethylenediamine-ZnO nanorods, (c) citrate-ZnO nanorods, (d) butanethiol-ZnO nanorods

In ECL spectra measurement, electron transfer reactions occurred between positively coreactants and negatively charged ZnO surface, resulted in the recombination of electron and hole on the ZnO contact surface and then led to the production of visible light. So ECL emission was characteristic of surface energy levels. The results indicated that the maximum ECL emission wavelength of ZnO sample decreased as surface modification was carried out, and the maximum ECL emission wavelength will also be influenced by the type of functional molecules. Because the point defect on the contact surface provides the active site of electrochemical luminescence and influences the position of deep energy level in Brillouin zone of ZnO, complexed structures formed on surface of ZnO nanorods as surface modification were carried out and led to the surface passivation of ZnO nanorods, which will influence the surface band gap of ZnO nanorods and then result in the change of ECL emission spectra.³⁶ For ZnO nanorods, the uppermost energy of the valence bands mainly consisted of O-based 2p orbits with a small mixing of Zn-based 3d orbits, where the bottom of the conduction bands is primarily assembled from the Zn-based 4s orbits with small contributions from O based 2p orbits and O based 2s orbital.³⁷ When Zn atoms on the surface of ZnO are bonded with $-NH_2$, the

top of the valence bands is dominated by the N 2p, O 2p, and Zn 3d states, whereas the bottom of the conduction bands comes from the Zn 4s states.⁴ The N 2p states hybridize with the Zn 3d states and then influence the level of the bottom of the conduction bands. For $-COO^-$ adsorbed ZnO nanorods, the energy of the edge of the valence band decreases when a monolayer is formed.³⁸ For ZnO nanorods modified with 1-butanethiol molecules, S atoms in 1-butanethiol molecules are cooperated with Zn atoms that presented on the surface of ZnO nanorods, the top of the valence bands is dominated by the mixture of the S 2p states and O 2p states, whereas the bottom of the conduction bands derive mainly from the Zn 4s states. The valence band maximum states come mainly from the S 2p and O 2p, whereas the conduction band minimum states are based on the S 2p and Zn 4s states.⁹ The variation of ECL spectra reflected the difference of surface state of functional ZnO nanorods, which resulted from the interaction between the surface atoms of ZnO and the functional groups in the adsorbed organic molecules to the influence of the bottom of the conduction bands and the top of valence bands.

Conclusion

In this work, three organic molecules were used to study the effect of functional molecule type to surface state of modifying ZnO nanorods. The results indicated that the maximum electrochemiluminescence emission wavelength decreased as ZnO nanorods were modified with ethylenediamine, sodium citrate and butanethiol. The variation of surface band gaps may originate from the difference of complexed structures and induces the difference of charge redistribution in the surface of ZnO nanorods anchored with different organic ligands. It contributes to an understanding of organic - inorganic interfaces and surface properties and may be useful for the design of novel multiplexing sensors or photovoltaic-hybrid materials and the corrosion prevention of ZnO nanostructures.

Acknowledgment

This work was supported by the National Natural Science Foundation of China (Grant No. 21075058, 21127006), Natural Science Foundation of Shandong Province (ZR2012BM007).

References

- Z. R. Tian, J. A. Voigt, J. Liu, B. McKenzie, M. J. McDermott, M. A. Rodriguez, H. Konishi and H. Xu, *Nat. Mater.*, 2003, 2, 821-826.
- J.-I. Hong, J. Choi, S. S. Jang, J. Gu, Y. Chang, G. Wortman, R. L. Snyder and Z. L. Wang, *Nano Lett.*, 2012, 12, 576-581.
- A. McLaren, T. Valdes-Solis, G. Li and S. C. Tsang, *J. Am. Chem. Soc.*, 2009, 131, 12540-12541.
- S.-P. Huang, H. Xu, I. Bello and R. Q. Zhang, *J. Phys. Chem. C*, 2010, 114, 8861-8866.
- C. G. Allen, D. J. Baker, J. M. Albin, H. E. Oertli, D. T. Gillaspie, D. C. Olson, T. E. Furtak and R. T. Collins, *Langmuir*, 2008, 24, 13393-13398.
- T. L. Bahers, T. Pauporté, F. d. r. Labat, G. g. Lefèvre and I. Ciofini, *Langmuir*, 2011, 27, 3442-3450.
- C. L. Perkins, *J. Phys. Chem. C*, 2009, 113, 18276-18286.
- A. L. Briseno, T. W. Holcombe, A. I. Boukai, E. C. Garnett, S. W. Shelton, J. J. M. Frechet and P. Yang, *Nano Lett.*, 2009, 10, 334-340.

9. S.-Z. Deng, H.-M. Fan, M. Wang, M.-R. Zheng, J.-B. Yi, R.-Q. Wu, H.-R. Tan, C.-H. Sow, J. Ding, Y.-P. Feng and K.-P. Loh, *ACS Nano*, 2009, 4, 495-505.
10. S. P. Garcia and S. Semancik, *Chem. Mater.*, 2007, 19, 4016-4022.
- 5 11. M. A. Garcia, J. M. Merino, E. Fernández Pinel, A. Quesada, J. de la Venta, M. L. Ruíz González, G. R. Castro, P. Crespo, J. Llopis, J. M. González-Calbet and A. Hernando, *Nano Lett.*, 2007, 7, 1489-1494.
12. L. Chen, J. Xu, J. D. Holmes and M. A. Morris, *J. Phys. Chem. C*, 2010, 114, 2003-2011.
- 10 13. J.-H. He, J.-J. Ke, P.-H. Chang, K.-T. Tsai, P. C. Yang and I. M. Chan, *Nanoscale*, 2013, 4, 3399-3404.
14. P. Ruankham, L. Macaraig, T. Sagawa, H. Nakazumi and S. Yoshikawa, *J. Phys. Chem. C*, 2007, 115, 23809-23816.
- 15 15. N. S. Norberg and D. R. Gamelin, *J. Phys. Chem. B*, 2005, 109, 20810-20816.
16. P. D. Cozzoli, A. Kornowski and H. Weller, *J. Phys. Chem. B*, 2005, 109, 2638-2644.
17. J. Wang, Y.-J. Lee and J. W. P. Hsu, *J. Phys. Chem. C*, 2014, 118, 18417-18423.
- 20 18. C.-F. Wang, Y.-T. Wang, P.-H. Tung, S.-W. Kuo, C.-H. Lin, Y.-C. Sheen and F.-C. Chang, *Langmuir*, 2006, 22, 8289-8292.
19. G. Kwak, M. Seol, Y. Tak and K. Yong, *The Journal of Physical Chemistry C*, 2009, 113, 12085-12089.
20. N. J. Nicholas, G. V. Franks and W. A. Ducker, *Langmuir*, 2012, 28, 7189-7196.
- 25 21. J.-H. Koo, J.-J. Cho, J.-H. Yang, P.-J. Yoo, K.-W. Oh and J.-H. Park, *Bull. Korean Chem. Soc.*, 2012, 33, 636-640.
22. X. G. Han, H. Z. He, Q. Kuang, X. Zhou, X. H. Zhang, T. Xu, Z. X. Xie and L. S. Zheng, *J. Phys. Chem. C*, 2009, 113, 584-589.
- 30 23. J. D. Kubicki, L. M. Schroeter, M. J. Itoh, B. N. Nguyen and S. E. Aplitz, *Geochim. Cosmochim. Acta*, 1999, 63, 2709-2725.
24. S. Sakohara, M. Ishida and M. A. Anderson, *J. Phys. Chem. B*, 1998, 102, 10169-10175.
25. S. Sakohara, L. D. Tickanan and M. A. Anderson, *J. Phys. Chem.*, 1992, 96, 11086-11091.
- 35 26. M. Nara, H. Torii and M. Tasumi, *J. Phys. Chem.*, 1996, 100, 19812-19817.
27. P. J. Thistlethwaite, M. L. Gee and D. Wilson, *Langmuir*, 1996, 12, 6487-6491.
- 40 28. P. J. Thistlethwaite and M. S. Hook, *Langmuir*, 2000, 16, 4993-4998.
29. J. Singh, J. Im, J. E. Whitten, J. W. Soares and D. M. Steeves, *Langmuir*, 2009, 25, 9947-9953.
30. A. B. Djurišić, W. C. H. Choy, V. A. L. Roy, Y. H. Leung, C. Y. Kwong, K. W. Cheah, T. K. Gundu Rao, W. K. Chan, H. Fei Lui and C. Surya, *Adv. Funct. Mater.*, 2004, 14, 856-864.
- 45 31. A. B. Djurišić, Y. H. Leung, K. H. Tam, L. Ding, W. K. Ge and W. K. Chan, *Nanotechnology*, 2007, 18, 095702.
32. A. B. Djurišić, Y. H. Leung, K. H. Tam, L. Ding, W. K. Ge, H. Y. Chen and S. Gwo, *Appl. Phys. Lett.*, 2006, 88, 103107.
- 50 33. Z. Ding, B. M. Quinn, S. K. Haram, L. E. Pell, B. A. Korgel and A. J. Bard, *Science*, 2002, 296, 1293-1297.
34. J. P. Wilcoxon, G. A. Samara and P. N. Provencio, *Phys. Rev. B Condens. Matter Mater. Phys.*, 1999, 60, 2704-2714.
35. Y. Gong, T. Andelman, G. Neumark, S. O'Brien and I. Kuskovsky, *Nanoscale Res. Lett.*, 2007, 2, 297-302.
36. Y. Bae, N. Myung and A. J. Bard, *Nano Lett.*, 2004, 4, 1153-1161.
37. L. Wang, Q. Yue, H. Li, S. Xu, L. Guo, X. Zhang, H. Wang, X. Gao, W. Wang, J. Liu and P. Liu, *Sci. China: Chem.*, 2013, 56, 86-92.
38. A. Lenz, L. a. Selegård, F. Söderlind, A. Larsson, P. O. Holtz, K. Uvdal, L. Ojamae and P.-O. Käll, *J. Phys. Chem. C*, 2009, 113, 17332-17341.
- 60